Radio Science, Volume 19, Number 6, Pages 1475–1484, November–December 1984

The middle and upper atmosphere radar: First results using a partial system

Susumu Kato, Toru Ogawa, Toshitaka Tsuda, and Toru Sato

Radio Atmospheric Science Center, Kyoto University, Uji, Japan

Iwane Kimura and Shoichiro Fukao

Department of Electrical Engineering, Faculty of Engineering, Kyoto University, Kyoto, Japan

(Received May 8, 1984; revised July 31, 1984; accepted July 31, 1984.)

The middle and upper atmosphere radar of Radio Atmospheric Science Center, Kyoto University, is now partly in operation. The facility will be complete in 1985. The active array antenna system of the radar makes it possible to steer the radar beam in an interpulse period, i.e., 400 μs. The antenna system consists of independently operative subgroups, each having 19 Yagis. We expect various sophisticated experiments by the system. A preliminary observation was successful to elucidate atmospheric motions during typhoon 5 which approached the radar site in August, 1983.

1. INTRODUCTION

The middle and upper atmosphere (MU) radar has been under construction at Shigaraki (35°N, 136°E) in the southeast of Kyoto since 1981. While the total system will be completed in 1985, the system is now, on a reduced scale, in operation for observation of the troposphere and lower stratosphere. In the present paper we shall first outline the MU radar system, which was improved from that originally designed in 1980 [*Fukao et al.*, 1980] and, later, present some observed results so far obtained.

2. SYSTEM OUTLINE

The MU radar is a pulse modulated monostatic Doppler radar with active antenna array working on the frequency of 46.5 MHz. The basic idea of the system design was discussed by *Fukao et al.* [1980]; the bandwidth is now given as 1.65 MHz, which allows us to have the 1-μs-wide pulse which gives the 150-m height resolution. In Table 1 the basic parameters are listed. Table 2 gives comparison of various VHF radars currently in operation. The block diagram of the system is illustrated in Figure 1. Figure 2 shows a recent photo of the MU radar system. The radar site is in hilly national forests and fairly well protected against radio noise interference.

Paper number 4S1062.
0048-6604/84/004S-1062$08.00

The radar antenna system consists of 475 antennas of three subelement crossed Yagi arrayed in a circular area with diameter of approximately 100 m (Figure 2). The array is divided into 25 subgroups (increased from 15 in the original 1980 design). Each subgroup consists of 19 elements which are on the equilateral triangular grids in each hexagon, the hexagon which makes up the main part of the antenna system (Figure 2*b*). Exception is for the six subgroups which are distributed just outside the hexagon areas and just inside the circular periphery, based on the triangular distribution. These groups are necessary for keeping the same antenna beam pattern in steering at any azimuth. This basic triangular distribution with an antenna at each apex of the equilateral triangle of its side 0.7λ long, where λ is the radar wavelength, is found to prevent grating lobes from appearing in the antenna beam steering if not exceeding 40° from the zenith [e.g., *Sato*, 1980]. Under such beam steering, the side lobe level for elevation angle less than 20° is suppressed smaller than −40 dB to the main lobe. The circular array has an effective area of 8330 m^2 producing the main beam of 3.6° in width. When the radar beam is directed vertically, the side lobe is symmetric about the main lobe, the first side lobe being as low as −18 dB to the main lobe. The crossed Yagi can produce two linear (mutually orthogonal) polarizations and also left-handed and right-handed polarizations.

A feature of the MU radar system is that each antenna element is activated by its own solid state power amplifier, its peak output power being 2.4

TABLE 1. Basic Parameters of the MU Radar

Parameter	Value
Location	Shigaraki, Shiga, Japan (34.85°N, 136.10°E)
Frequency	46.5 MHz
Antenna configuration	circular array of 475 crossed Yagi antennas
Aperture	8330 m^2 (103 m in diameter)
Beam width	3.6° (one-way, half power)
Polarizations	linear or circular
Beam directions	0°–30° zenith angle
Steerability	steering is completed in IPP
Transmitter	
Power amplifier	475 solid-state amplifiers, each output being 2.4 KW peak and 120 W average
Peak power (system)	1 MW
Average power (system)	50 KW (duty ratio 5%)
Bandwidth	1.65 MHz max (pulse length: 1–512 μs variable)
IPP	400 μs min
Receiver	
Bandwidth	1.65 MHz maximum
Dynamic range	70 dB
IF	5 MHz
Modulator	Binary phase-coding of the 32-bit length of pulse as the maximum, Barker and Complementary codes being used at present
A/D converter	12 bits × 4 channels

KW. Since the total number of the antenna is 475, the total peak output power becomes approximately 1 MW allowing for antenna loss. Each antenna has also its own receiver preamplifier. Both transmitter power amplifier and receiver preamplifier are mounted on transmitter-receiver (TR) module (14 cm × 70 cm × 55 cm). Each of the six booths near the antenna accommodates the modules of four subgroups, i.e., (19 × 4) modules except for one booth which accomodates the modules of five subgroups, i.e., (19 × 5) modules. Conversion between the 46.5 MHz radar frequency and the 5 MHz IF frequency, for transmission and reception, takes place in the modules, thereby making use of the IF for the signal transfer between the booth near the antenna and the control building on the hill (Figure 2).

TABLE 2. Comparison Among VHF Radars Currently in Operation for Atmospheric Observation

Facility	Location	Frequency, MHz	Average Power × Aperture, Wm^2	Beam Width, deg	Antenna Configuration	Reference
Altair	Kawajalein	155	1.8×10^6	2.8	steerable dish	*Balsley and Gage* [1980]
EISCAT	North Scandinavia	224	2.0×10^9	1.7 × 0.6	steerable parabolic cylinder	*Folkestad et al.* [1983]
Jicamarca	Peru	49.9	2.0×10^{10}	1.0	phased dipole array	*Balsley and Gage* [1980]
MU	Japan	46.5	5.0×10^8	3.6	phased Yagi array	
Platteville	Colorado	49.9	4.5×10^6	3 × 3	phased dipole array	*Balsley and Gage* [1980]
Poker Flat	Alaska	49.9	2.6×10^9	1.1, two-way	phased dipole array	*Carter and Balsley* [1982]
SOUSY (stationary system)	Germany	53.5	7.6×10^7	5	phased Yagi array	*Czechowsky et al.* [1984]
SOUSY (mobile system)	Germany	53.5	7.1×10^7	3	phased Yagi array	*Czechowsky et al.* [1984]
Sunset	Colorado	40.5	9.4×10^6	5 × 9	phased dipole array	*Balsley and Gage* [1980]
Urbana	Illinois	40.9	8.8×10^7	3.6 × 4.8	phased dipole array	*Tanner et al.* [1982]

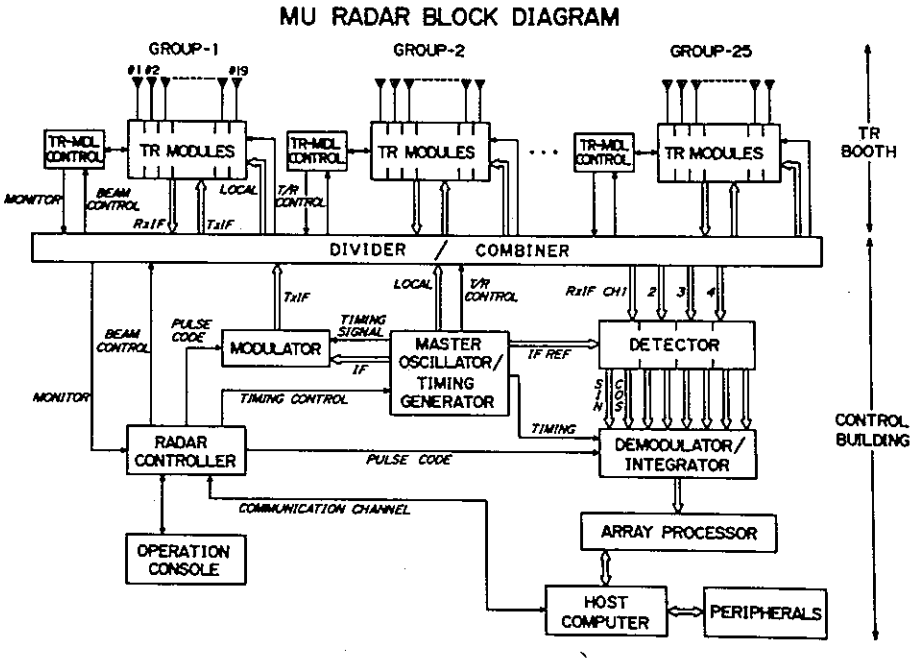

Fig. 1. Block diagram of the MU radar system. The radar controller (HP 9835A) basically controls all parts of the system, both in the control building and the booths. Computer (VAX 11/750) is used for data analysis (as calculating various spectral moments) and data-taking, and for controlling an array processor (MAP 300) which works for calculation of FFT and ACF, and incoherent integration; TR module control is done by 25 microprocessors; the received signal can be processed in four channels, each for sine and cosine detection; the basic signal generator uses a rubidium vapor frequency standard.

The main advantage of this active array system is that the phase of the signal transmitted from each antenna required for the beam steering is electronically controlled at low power level. The beam can be tilted to as many locations as 1657 within 30° from the zenith for each interpulse period (IPP, hereafter), i.e., as short as 400 μs. Thus, it is possible to observe the fast varying dynamic behavior of the atmosphere, e.g. gravity waves with fairly short periods.

Each independently operative antenna subgroup enables various sophisticated observations as that of the close spaced antenna method [e.g., *Briggs*, 1980] which detects propagation of the interference pattern among the signals received at each antenna.

In order to increase the signal-to-noise ratio without losing the height-resolving power, the pulse compression can be used in the MU radar system. In the pulse compression one can generate various binary-coded pulses with its length up to 32 bits. At present both Barker and Complementary codes are actually used for observation of the troposphere and stratosphere. The complementary code gives zero sidelobe for the autocorrelation and suits the troposphere and middle atmosphere observation where the radar echo correlation time is much longer than IPP, suitable for transmitting a pair of the complementary-coded pulse [e.g., *Woodman*, 1980].

As to the data processing, for coherent integration we use an integrator to be able to process up to 1024 complex samples of data in IPP; the maximum number of addition is 128 (Figure 1). Further, Doppler spectrum and autocorrelation function of the samples are obtained by an array processor (MAP 300) which is controlled by a host computer (VAX 11/750). Averaging of the result is also done by this array processor. The host computer works for calculation of physical parameters and writing into MT.

The system now in operation is on a reduced scale as having three subgroups (57 antennas) which are transmitting, approximately, the 120 kW pulse in the 10°-wide beam. This system is, however, complete in other parts as in controlling, modulation, demodulation and signal-processing, all of which are installed in the control building (Figure 1). We have already confirmed various operations of the present system. Figure 3 illustrates an observation in which the beam

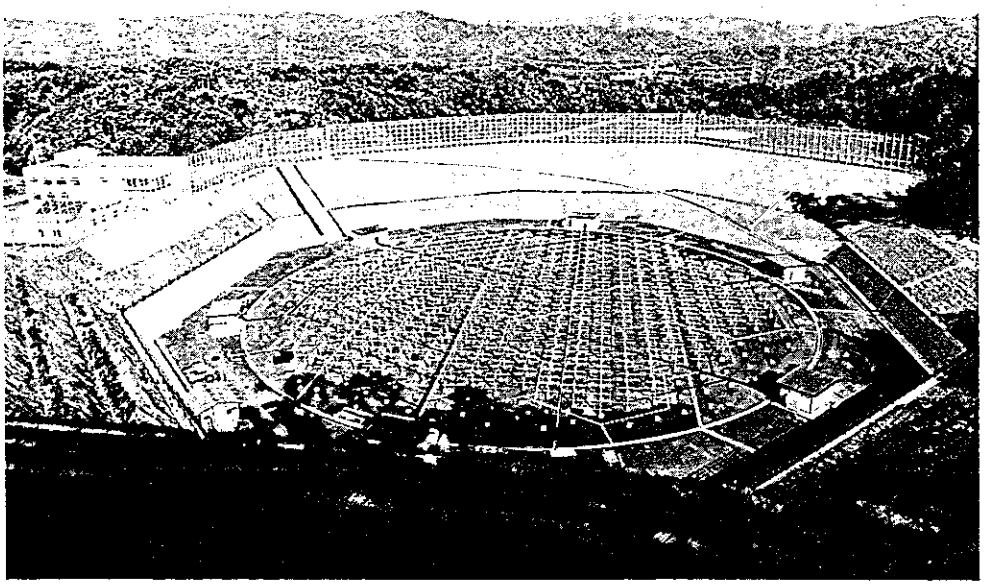

Fig. 2*a*. Bird's-eye view of the MU radar system. The circular antenna area is marked by white paint line, along and just outside of which the six booths are distributed; each subgroup of the antenna corresponds to each hexagon or each peripheral region as marked by white paint, solid or broken lines, the solid line showing the territorial boundary of each booth; the booth and the antenna element being connected by coaxial cables extended along the surface; the antenna level is lower by 15 m than the surrounding hill on which the iron net fence of 10 m high is built, mainly for avoiding the ground clutter due to the side lobe radiation in low elevation angle; the two-storied building on the left on the hill is control building and, next door is the guest house; the white circle just beyond the fence on the right is a heliport.

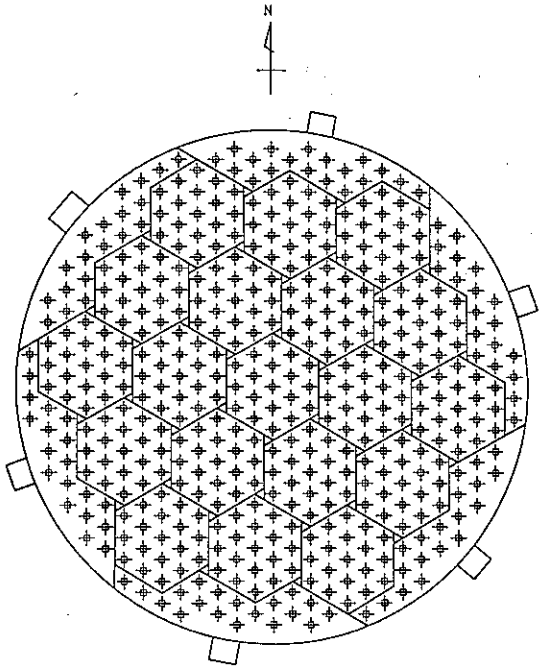

was steered azimuthally, keeping it in a constant zenith angle of 30° (velocity azimuth display (VAD) method; *Balsley and Farley* [1976]). The beam was steered in every interpulse period. Figure 3*a* illustrates the contour map of observed Doppler spectra versus height. The map varies with the radar beam direction as expected. Apparent echoes at zero Doppler velocity were mainly due to a system fault, a weak leakage of transmission; we expect quick correction to the fault. The 16-bit complementary-coded pulse was used, each subpulse being 1 μs wide. The

Fig. 2*b*. (Opposite) Antenna array of the MU radar. The small cross is a Yagi which is crossed three elements for independent two linear waves, and right-handed and left-handed polarization waves. The small square at each small cross is a concrete block for the antenna foundation. The hexagon is the basic unit of the antenna system, consisting of 19 Yagi's. In between the hexagon area and the circular boundary there are 6 groups of antenna; each group also consists of 19 Yagi's. The six boxes around and just oustide the antenna area are booths which accommodate transmitter-receiver modules.

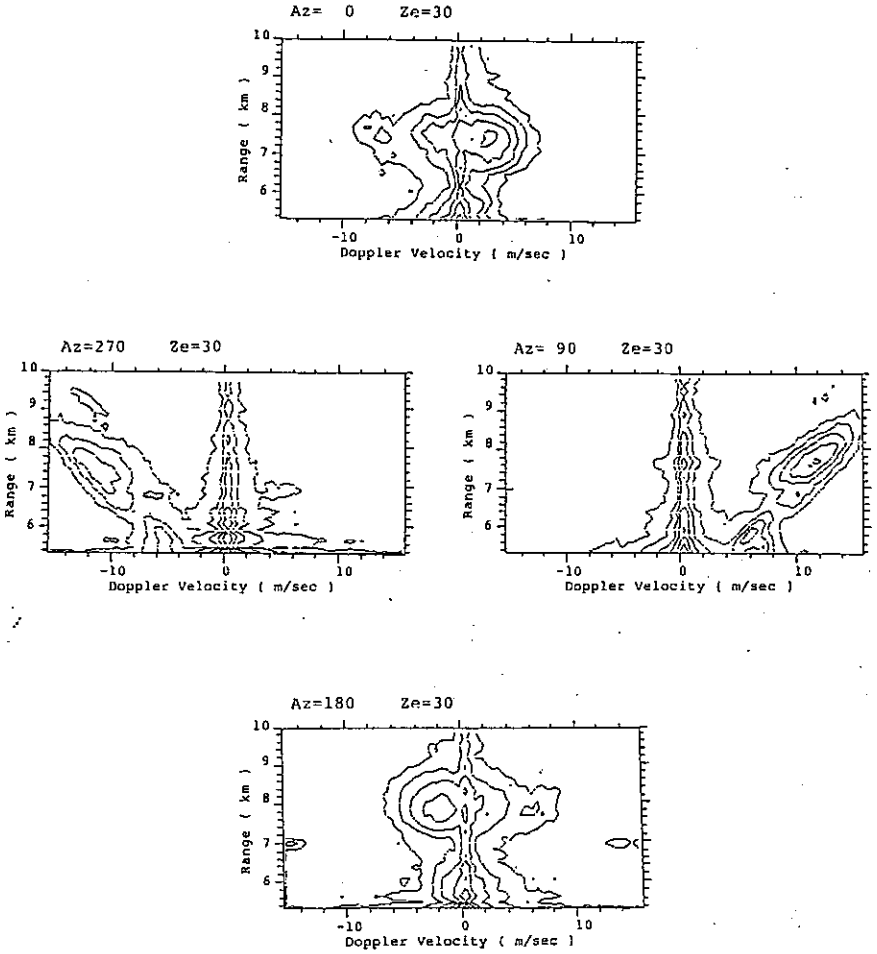

Fig. 3*a*. VAD observation. Height distribution of Doppler spectrum of line-of-sight velocity is shown as contour map; positive for leaving and negative for approaching the facility. Each beam steering was completed during an interpulse period even as short as 400 μs for the 16-bit complementary code with the 1-μs-wide subpulse; the antenna zenith angle was kept at 30° and the azimuth angle changed, from the north, by 25° or 20° in every other swinging, completing 16 observations in one round; two consecutive rounds are required to finish one observation set for a pair of complementary codes. After coherent integration of 16 sweeps, FFT was done on 128 points. A system fault produced erroneous echoes at zero Doppler velocity.

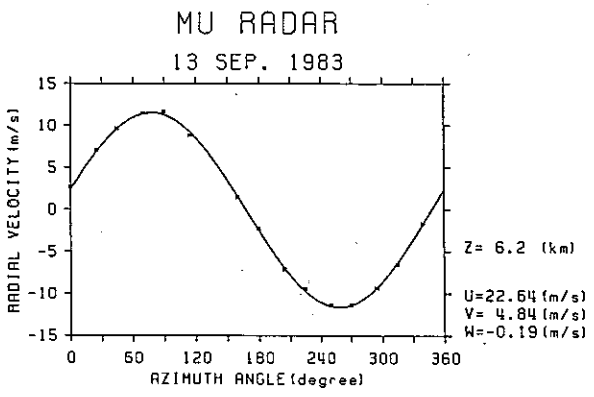

Fig. 3*b*. (Opposite) Line-of-sight (radial) velocity at 6.2 km varying with azimuth; the observed value (small cross) follows well the expected sinusoidal curve (solid curve) giving the wind velocity U (eastward), V (northward) and W (upward) as shown.

minimum delay for receiving the echo was thus 16 μs due to the total pulse length plus 20 μs due to the system recovery. This overall 36 μs delay made the minimum observable range 5.4 km as in the maps. The contour spacing is 4.0 dB (top), 5.0 dB (middle, left), 5.1 dB (middle, right) and 5.8 dB (bottom). Note that the spectrum broadens a little due to the truncation of data in time series in the analysis [*Sato and Woodman*, 1982]. The observed velocity V_r is line-of-

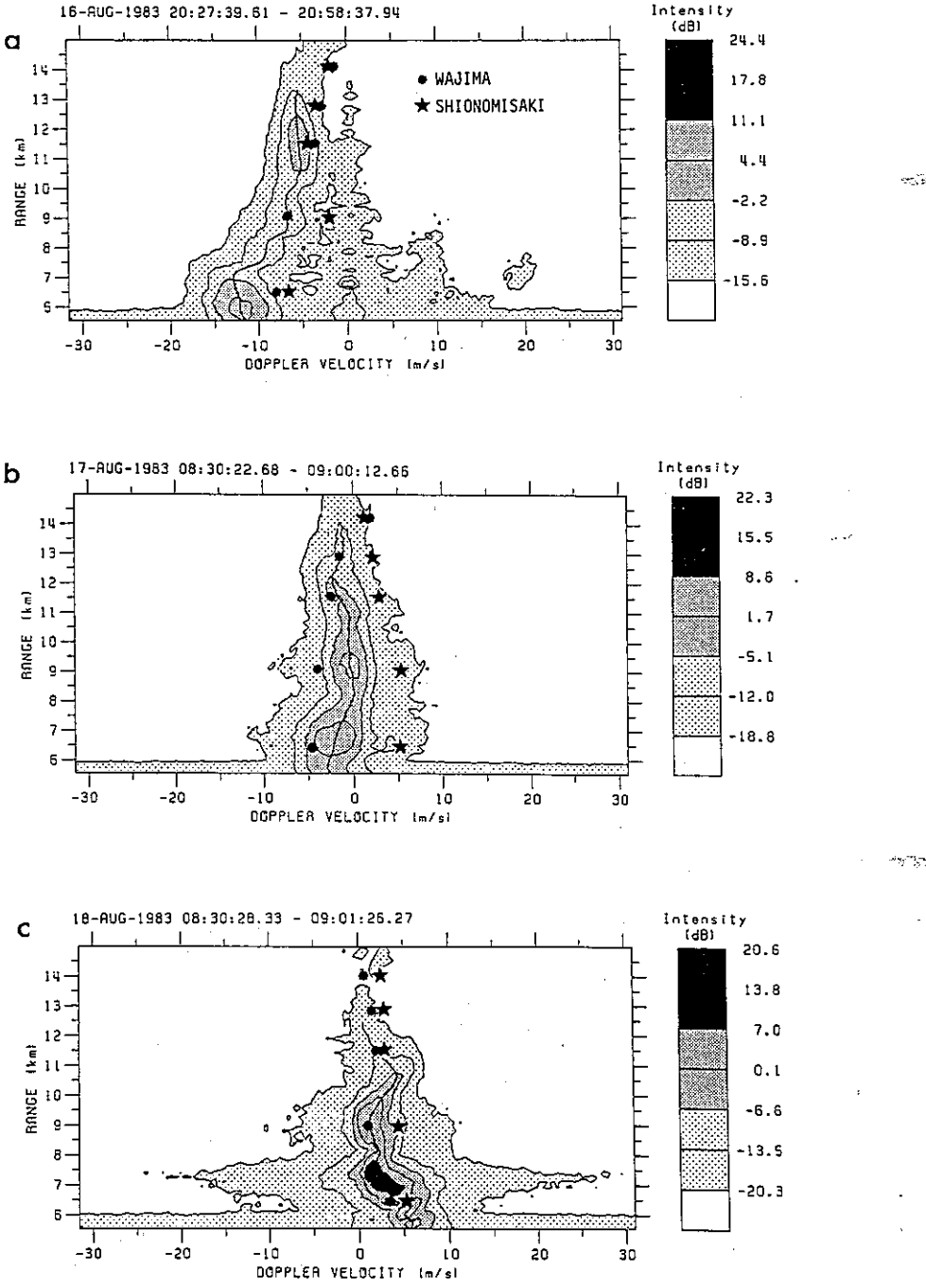

Fig. 4. Doppler spectrum of the line-of-sight wind velocity for the 30° tilting from the zenith toward the east. Contour is subject to the dB scale as shown beside the main diagram. The dark asterisk denotes observation at Shionomisaki and the circle at Wajima. (*a*) Average for 2028–2059 Aug. 16. Erroneous echoes appear around the zero-doppler velocity as in Figure 3*a*. An image of the doppler at −10m/s occurs (at 10m/s) due to an unbalanced sine and cosine detection, a failure which was improved later. (*b*) Average for 0830–0900 Aug. 17. (*c*) Average for 0830–0901 Aug. 18. The apparent widening of spectrum as in Figure 3*a* is due to the weak level trail which results from truncation errors of data [*Sato and Woodman*, 1982]. Note that the real variance is only a few m/s. The minimum observed range is also 5.4 as in Figure 3*a*.

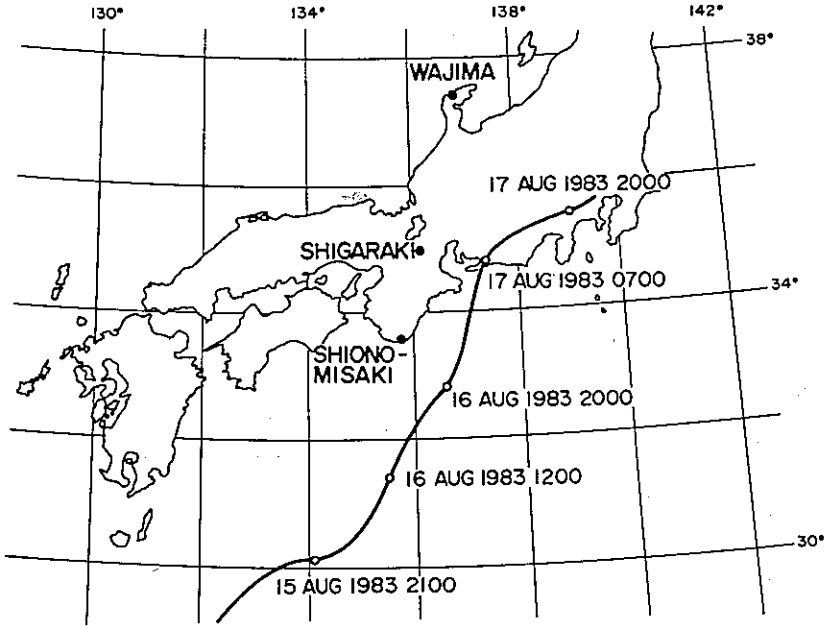

Fig. 5. Path of typhoon 5. The thick solid line shows the typhoon path. The three small circles on the path are the location of the typhoon center on August 15 (21 h), 16 (20 h) and 17 (20 h), respectively. The center movement was as slow as 18 km/hr.

sight components along the radar beam as given,

$$V_r = (U^2 + V^2)^{1/2} \sin \Theta \cos (\phi + \arctan V/U) + W \cos \Theta \quad (1)$$

where U, V, and W are eastward, northward and upward components of the wind vector, respectively, Θ is the zenith angle and ϕ the azimuth angle. If the wind remains constant during observation (0.1 s), (1) shows that V_r varies sinusoidally with a constant term $W \cos \Theta$. Figure 3 suggests that this is almost the case, giving U, V, W as shown beside the diagram.

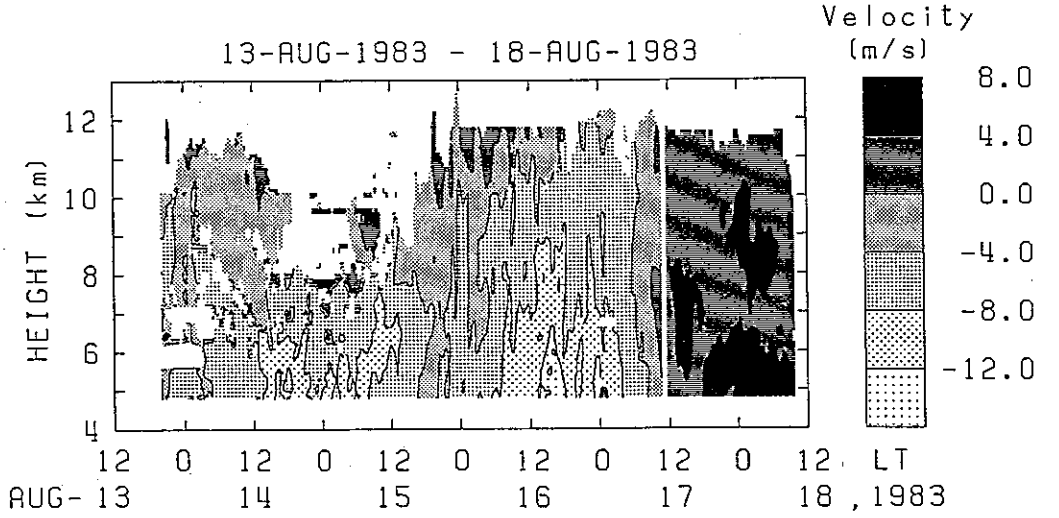

Fig. 6. Line-of-sight (tilted toward the east by 30° from the zenith) wind velocity distribution varying with time during typhoon passage. Contour is subject to meters per second shown in the column beside the diagram.

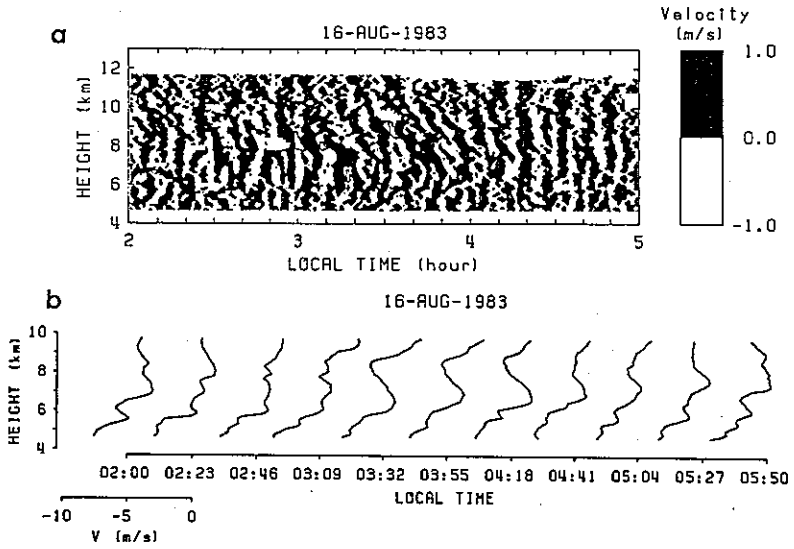

Fig. 7. Fluctuating winds in typhoon 5. (*a*) Contour distinguishes between positive and negative velocity regions; averaged values for 1 min are used, removing longer period components than 10 min. (*b*) Height profiles at various times; averaged values for 23 min are used.

3. OBSERVATION OF THE TROPOSPHERE AND THE LOWER STRATOSPHERE DURING TYPHOON 5 IN 1983

Since April, 1983, we have been attemping to measure the wind velocity between 4 and 15 km in height on many occasions using the three subgroups which are now complete. Observation is limited only for period with no construction work to complete the rest of antenna system.

Figure 4 shows some result of observation in August, 1983 when typhoon 5 approached Japan as shown in Figure 5. The observation was done using the complementary code of 16 bits of the 1 μs subpulse, the pulse repetition frequency of 2.5 kHz; after 128-times coherent integration (51.2 ms) of orthogonally detected signals, 128-point FFT was carried out. For the purpose of smoothing an averaging was done on 10 of the results. This implies an observation at each level approximately in 1 min. The sampled levels were 64 in number between 4 km and 15 km from the ground. In Figure 4 further averaging is done for approximately 30 min. The antenna beam was tilted by 30° from the zenith toward the east, positive for leaving and negative for approaching the facility. Note that since the vertical velocity averaged for 30 min should be much smaller than the horizontal at Shigaraki which was at least 100 km distant from the typhoon center, the positive and negative values correspond to eastward wind (westerly) and westward wind (easterly), respectively. It is clear that the wind observed by the MU radar is consistent with that observed by the conventional radiosonde at Wajima and Shionomisaki considering the location of the typhoon; the distance between Shionomisaki and Shigaraki is about 150 km and that between Shigaraki and Wajima 250 km. The wind velocity distribution with height was obtained from the spectral peak at each altitude and the distribution changed with the typhoon location relative to Shigaraki, as is expected. Figures 4*a*, 4*b* and 4*c* give such features where one can readily find the wind field to have returned to normal, i.e., a westerly when the typhoon receded from Shigaraki. The overall wind distribution varying with time is shown in Figure 6.

Further analysis of the data for typhoon 5 has revealed an existence of temporal fluctuation of the wind as shown in Figure 7*a* where the contour map (top) distinguishes between positive and negative velocity regions; the data used are those obtained approximately in 1 min and filtered to pick up only shorter period components than 10 min. The period of fluctuation is around several minutes, which corresponds to the Brunt-Väisälä frequency. The observation was done only for one direction, 30° from the zenith toward the east. No information was available about the fluctuating wind vector. Figure 7*b* shows height profiles of the line-of-sight wind velocity averaged over 23 min.

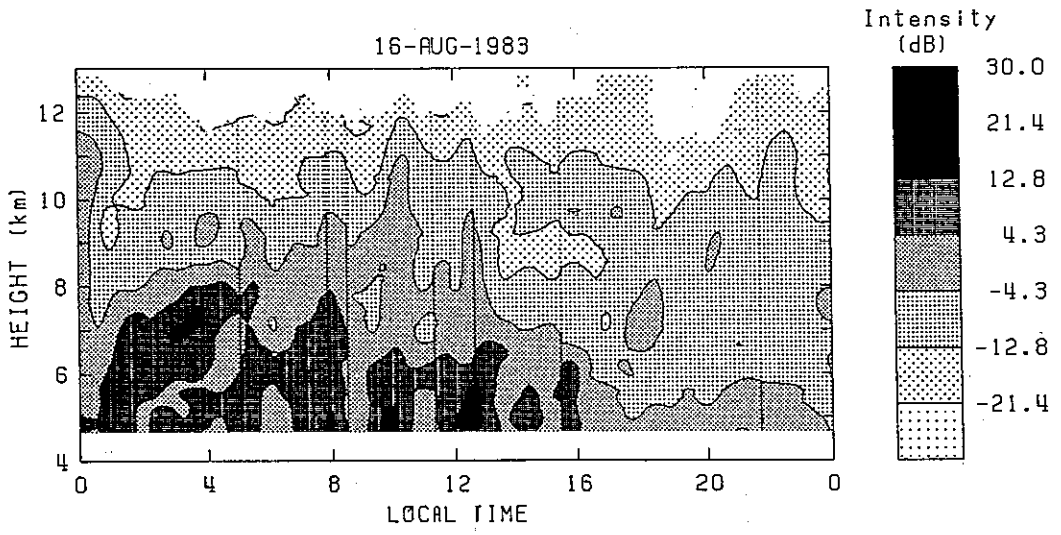

Fig. 8. Echo power during typhoon 5. The contour corresponds to relative intensity in dB as given by the scale beside the diagram. Intense echo occurs around 7 km height first, descending with time.

4. DISCUSSION

The MU radar is now in operation on a reduced scale. However, as is shown in section 3, we have already been successful in the observation of typhoon detecting some of its temporal dynamical behavior varying with altitudes.

Figure 4*a* shows that typhoon 5 produced strong westward winds on the left-hand side to the direction of the typhoon course, its intensity attaining as strong as 20 m/s near Shigaraki distant from the typhoon center by about 250 km, then decreasing with distance, yet still detectable at Wajima distant about 520 km; the observed wind, at this time, at Shionomisaki, was weaker partly because of its location which is more deflected to the west than that of Shigaraki relative to the typhoon. Such effects of the typhoon as reversing the usually present weak westerly were very remarkable at the lowest level observed. But the effects became weaker with height. When typhoon 5 moved further north-eastward and reached the east side of Shigaraki (Figure 4*b*), the typhoon effect became very weak on the zonal wind as is expected; considering the anticlockwise spiral wind into the typhoon center, the typhoon then should produce mainly southward winds. This is much more remarkable at Shionomisaki (Figure 4*b*), where the typhoon effect had almost disappeared as understood from comparison of the observation there between Figure 4*b* and Figure 4*c*. At this time Wajima is most disturbed by the typhoon. However, the general situation is unclear because of no data for meridional winds at all. Nevertheless, a dynamic behavior of typhoon 5 seems to be fairly clearly demonstrated by the MU radar as in Figures 4*a*–4*c*. Because of continuous wind-probing, the facility will play a role in the typhoon monitor for practical purposes in future.

Severe weather activity as typhoons and intense tornadoes has been suspected to be a generator of gravity waves which propagate upward to the ionosphere, producing medium scale traveling ionosphere disturbances (MS TID's) [e.g., *Tsutsui and Ogawa*, 1973; *Francis*, 1974; *Huang et al.*, 1978]. Some meteorological observations have also been carried out to detect gravity waves with long periods as a few hours in association with severe convective storms [*Uccellini*, 1975]. The present observation as in Figure 7 would be novel in that it is a direct wind observation during typhoon giving the wind profile with height with good time resolution of 1 min. The contour pattern in Figure 7*a* recurs with a period of about 7 min. At this height the phase progresses both upward and downward as in Figure 7*a*. The radar echo from this height was found intense, as in Figure 8, showing an existence of intense turbulence. A strong wind shear may excite both the intense turbulence and the Brunt-Väisälä oscillation, although no evidence for such wind shear was found in the averaged wind profile in Figure 6. Fast varying wind can produce the shear. Note that similar wind oscillation was detected at similar height by *Klostermeyer and Rüster* [1981] in the presence of the jet stream

producing a strong wind shear. Since our observation was only for one direction, 30° from the zenith toward the east, the situation remains inconclusive on the excitation of the observed fluctuation. Another drawback of the present observation is the fact that, while the pulse width used in the observation is as short as 1 μs, the beam width of the present small system is as wide as 10°, yielding the height resolution as only 1 km, a resolution which is not enough to decide the phase variation very precisely in Figure 7. In atmosphere dynamics it is important to study three-dimensional wind fluctuation during typhoons under better height resolution.

Acknowledgments. The MU radar was designed under financial support by Science Grant for Unified Research B 1976 and 1977 and by A 1978 Ministry of Education, Science and Culture Japan. The present observation is also supported partially by Science Grant for Unified Research A 1983 and 1984 and by that for General Research B 1982, 1983 and 1984. Partial support is further given to the present work by the Nissan Science Foundation 1981–1983. The present authors are indebted much to many graduate students, Department of Electrical Engineering and Electronics, Kyoto University, such as M. Okumura, Y. Ayaki, T. Nishida and S. Morimoto. They have assisted the present authors in designing the radar system, developing the operation softwares and participating in the present observations. Cooperation of K. Wakasugi, Kyoto Institute of Technology, in solving various technical problems of the MU radar system, is also much appreciated.

REFERENCES

Balsley, B. B., and D. T. Farley, Auroral zone winds detected near the tropopause with Chatanika UHF Doppler radar, *Geophys. Res. Lett.*, *3*, 525–528, 1976.

Balsley, B. B., and K. S. Gage, The MST radar technique: Potential for middle atmosphere studies, *Pure Appl. Geophys.*, *118*, 452–493, 1980.

Briggs, B. H., Radar observation of atmospheric winds and turbulence: A comparison of techniques, *J. Atmos. Terr. Phys.*, *42*, 823–833, 1980.

Carter, D. A., and B. B. Balsley, The summer wind field between 80 and 93 km observed by the MST radar at Poker Flat, Alaska (65°N), *J. Atmos. Sci.*, *39*, 2905–2915, 1982.

Czechowsky, P., G. Schmidt, and R. Rüster, The mobile SOUSY Doppler radar: Technical design and first results, *Radio Sci.*, *19*, 441–450, 1984.

Folkestad, K., T. Hagfors, and S. Westerlund, EISCAT: An updated description of technical characteristics and operational capabilities, *Radio Sci.*, *18*, 869–879, 1983.

Francis, S. H., A theory of medium-scale ionospheric disturbances, *J. Geophys. Res.*, *79*, 5245–5260, 1974.

Fukao, S., S. Kato, T. Aso, M. Sasada, and T. Makihira, Middle and upper atmosphere radar (MUR) under design in Japan, *Radio Sci.*, *15*(2), 225–231, 1980.

Huang, R. J., T. Phan, and R. E. Smith, Observation of gravity waves during the extreme tornado outbreak of 3 April 1974, *J. Atmos. Terr. Phys.*, *40*, 831–843, 1978.

Klostermeyer, J., and R. Ruster, Further study of a jet stream–generated Kelvin-Helmholz instability, *J. Geophys. Res.*, *86*, 6631–6637, 1981.

Sato, T., Coherent radar measurement of the middle atmosphere and design concepts of MU radar, Ph.D. thesis, Dep. of Electr. Eng., Kyoto Univ., Kyoto, Japan, 1980.

Sato, T., and R. F. Woodman, Fine-altitude-resolution radar observations of upper-tropospheric and lower-stratospheric winds and waves, *J. Atmos. Sci.*, *39*, 2539–2545, 1982.

Tanner, D. R., P. E. Mayes, and S. A. Bowhill, Phased array design including consideration of mutual coupling with application to the Urbana coherent-scatter radar, *Aeron. Rep. 108*, Univ. of Ill., Urbana, Ill., December 1982.

Tsutsui, M., and T. Ogawa, HF doppler observation of ionospheric effects due to typhoons, *Rep. Ionos. Space Res. Jpn.*, *27*, 121–123, 1973.

Uccellini, L. W., A case study of apparent gravity wave imitation of severe convective storms, *Mon. Weather Rev.*, *103*, 497–513, 1975.

Woodman, R. F., High-altitude resolution stratospheric measurement with the Arecibo 430-MHz radar, *Radio Sci.*, *15*, 417–422, 1980.

S. Fukao and I. Kimura, Department of Electrical Engineering, Faculty of Engineering, Kyoto University, Kyoto 606, Japan.

S. Kato, T. Ogawa, T. Sato, and T. Tsuda, Radio Atmospheric Science Center, Kyoto University, Gokanosho Uji, Kyoto 611, Japan.